Eur. Phys. J. D **7**, 107–116 (1999)

THE EUROPEAN PHYSICAL JOURNAL D

EDP Sciences

Effective mass in quantum effects of radiation pressure

M. Pinard[a], Y. Hadjar[b], and A. Heidmann[c]

Laboratoire Kastler Brossel[d], Case 74, 4 place Jussieu, 75252 Paris Cedex 05, France

Received: 21 January 1999

Abstract. We study the quantum effects of radiation pressure in a high-finesse cavity with a mirror coated on a mechanical resonator. We show that the optomechanical coupling can be described by an effective susceptibility which takes into account every acoustic modes of the resonator and their coupling to the light. At low frequency this effective response is similar to a harmonic response with an effective mass smaller than the total mass of the mirror. For a plano-convex resonator the effective mass is related to the light spot size and becomes very small for small optical waists, thus enhancing the quantum effects of optomechanical coupling.

PACS. 42.50.Dv Nonclassical field states; squeezed, antibunched, and sub-Poissonian states; operational definitions of the phase of the field; phase measurements – 42.50.Lc Quantum fluctuations, quantum noise, and quantum jumps – 43.40.+s Structural acoustics and vibration

Radiation pressure exerted by light plays an important role in quantum limits of very precise optical measurements. Quantum noise in interferometers has two fundamental sources, the photon noise of the laser beam and the fluctuations of the mirror's position due to radiation pressure. Both lead to a quantum limit for measurement sensitivity and potential applications of squeezed states have motivated a large number of works in quantum optics [1,2].

When a movable mirror is exposed to a laser beam, its position is coupled to the laser intensity via radiation pressure [3]. This *optomechanical coupling* may be enhanced using a high-finesse optical cavity that is very sensitive to small mirror displacements. Such a device is equivalent to cavities containing a Kerr medium and it has been studied for squeezing generation [4–7] or quantum non-demolition measurements [8–10].

Theoretical calculations of these effects are usually based on a description of the mechanical motion as a single harmonic oscillator. This model is well adapted to the motion of the center of mass for suspended mirrors, such as the ones of gravitational-wave antennas [11,12]. Radiation pressure can, however, excite internal acoustic modes of the mirror for which a simple description as a harmonic oscillator is not appropriate. These internal vibrations induce a deformation of the mirror which can be coupled to the light.

In this paper, we study the effect of optomechanical coupling on quantum fluctuations when internal acoustic modes of the mirror are considered. We show that the coupling can be described by an effective response of the mirror which takes into account all acoustic modes and their spatial matching with the light. Similar results have been obtained for the Brownian motion of mirrors which has been studied for gravitational-wave interferometers [13–16]. We show that the same effective response describes both thermal and radiation pressure effects. This response can be approximated to a harmonic response at low frequencies and the effective mass of this equivalent pendulum can be much smaller than the total mass of the mirror. This small effective mass enhances the quantum effects of optomechanical coupling.

The system studied in this paper is sketched in Figure 1. It consists of a single-port cavity with a movable mirror coated on the plane side of a mechanical resonator. The geometry of the resonator determines the spatial structure of the acoustic modes. The model presented in this paper is however valid for any geometry. We first recall the basic properties of the optomechanical coupling using a simple description in which both the field and the mechanical resonator are treated as one-dimensional objects and the mirror motion is described as a harmonic oscillator (Section 1).

We then study the effect of internal acoustic modes by taking into account the spatial structure of both the light and the resonator. We first determine the effect of a deformation of the resonator on the light field (Section 2). We then study the mechanical motion of the resonator when

[a] e-mail: pinard@spectro.jussieu.fr
[b] e-mail: hadjar@spectro.jussieu.fr
[c] e-mail: heidmann@spectro.jussieu.fr
[d] Laboratoire de l'Université Pierre et Marie Curie et de l'Ecole Normale Supérieure associé au Centre National de la Recherche Scientifique.

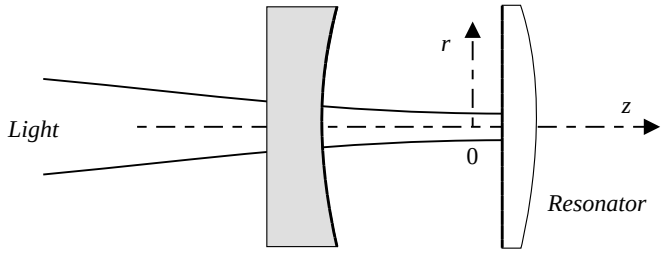

Fig. 1. Model of a Fabry-Perot cavity with a movable mirror. The mirror is coated on the plane side of a plano-convex mechanical resonator.

its plane side is submitted to the radiation pressure of the intracavity field. We finally define an effective susceptibility which describes the optomechanical coupling between the light beam and the resonator (Section 3). To illustrate the quantum effects of radiation pressure we study the quantum noise reduction of the field reflected by the cavity (Section 4).

We apply these results in the last section to the case of a plano-convex resonator (Section 5). Acoustic modes are then confined near the central axis of the resonator and their spatial structure can be described by analytical expressions which are quite similar to Gaussian optical modes of a Fabry-Perot cavity. We show that this geometry leads to a drastic reduction of the effective mass.

1 One-dimensional model of optomechanical coupling

We recall in this section the basic properties of the optomechanical coupling. For this purpose we neglect the internal motion of the resonator and we assume that the mirror moves without any deformation of its surface. The light is only sensitive to the mirror motion in the z-direction (Fig. 1) and this motion can be completely characterized by the position $z(t)$ of the mirror at time t.

The effect of the mirror motion on the intracavity field is a phase shift ψ related to the change of the optical path followed by the light

$$\psi(t) = 2kz(t), \tag{1}$$

where k is the wave vector of the light. The cavity detuning thus depends on the cavity length and couples the field to the mirror motion.

For small mirror displacements, the linear response theory shows that the Fourier transform $z[\Omega]$ of the mirror position is proportional to the applied force [17]

$$z[\Omega] = \chi[\Omega](2\hbar k I[\Omega] + F_{\mathrm{T}}[\Omega]), \tag{2}$$

where χ is the mechanical susceptibility of the mirror. If we assume that the mechanical motion is harmonic, this susceptibility has a Lorentzian shape

$$\chi[\Omega] = \frac{1}{M(\Omega_{\mathrm{M}}^2 - \Omega^2 - i\Omega_{\mathrm{M}}^2\Phi[\Omega])}, \tag{3}$$

where M is the mass of the mirror and Ω_{M} its resonance frequency. The loss angle $\Phi[\Omega]$ characterizes the damping of the motion and is related to the quality factor Q of the resonance by $\Phi[\Omega_{\mathrm{M}}] = 1/Q$. The first force in (2) represents the radiation pressure exerted by the intracavity field. It is proportional to the momentum exchange $2\hbar k$ during a photon reflection and to the light intensity I normalized as the number of photons reflected on the mirror by unit time. The second force F_{T} is a Langevin force describing the coupling of the resonator with a thermal bath. Its spectrum $S_{\mathrm{T}}[\Omega]$ is related to the mechanical susceptibility by the fluctuation-dissipation theorem [17]

$$S_{\mathrm{T}}[\Omega] = -\frac{2k_{\mathrm{B}}T}{\Omega}\mathrm{Im}\left(\frac{1}{\chi[\Omega]}\right), \tag{4}$$

where T is the temperature and k_{B} the Boltzmann constant.

Equation (2) shows that the radiation pressure exerted by the light couples the mirror motion to the light intensity. The mean effect of this coupling is a mean displacement $\overline{z}$ obtained from equation (2) by a statistical average of $z[\Omega = 0]$. From equation (1) this leads to a non-linear phase shift for the mean field in the cavity equal to

$$\psi_{\mathrm{NL}} = 4\hbar k^2 \chi[0]\,\overline{I}, \tag{5}$$

where $\overline{I}$ is the mean intracavity intensity. This intensity-dependent phase shift is equivalent to an optical Kerr effect. The cavity with a movable mirror is thus equivalent to cavities containing a Kerr medium which have been studied for squeezing generation [18–20] or QND measurements [21,22]. The main differences with a pure Kerr medium are due to the dynamics of the moving mirror characterized by the frequency dependence of the susceptibility $\chi[\Omega]$ and to the presence of thermal noise.

The non-linear phase shift ψ_{NL} is an important parameter to determine the efficiency of the optomechanical coupling. Quantum effects are significant if this phase shift is of the order of the cavity losses [10]. In this case the displacement $\overline{z}$ induced by the mean radiation pressure is of the order of the width $\lambda/\mathcal{F}$ of the cavity resonance (λ is the optical wavelength and $\mathcal{F}$ is the cavity finesse). This condition actually corresponds to the observation of bistability in the cavity. As usual in quantum optics, quantum effects are important near the bistability turning points. This condition depends on the optical characteristics of the system, such as the cavity finesse or the light intensity. It also depends on the mechanical properties of the resonator (Eq. (5)). In particular, quantum effects induced by optomechanical coupling are inversely proportional to the mass of the resonator.

2 Light reflexion on a moving mirror

We have shown in the previous section that the optomechanical coupling is based on two complementary effects. The first one is the phase shift of light induced by the mirror motion. The second effect is that the mirror moves in

response to radiation pressure. We examine in this section the first effect when internal modes of the resonator are taken into account.

Light is sensitive only to longitudinal displacements of the mirror. A longitudinal deformation of the plane side of the resonator can be described by its displacement $u(r, z = 0, t)$ in the z-direction at every radial point r of the surface (the origin of the cylindrical coordinates is taken at the center of the mirror, see Fig. 1). The electric field in front of the moving mirror can be written as

$$E(r,t) = v_0(r)\,\alpha(t)\,e^{-i\omega_0 t}, \tag{6}$$

where $\alpha(t)$ is the slowly varying amplitude of the field, ω_0 the optical frequency and $v_0(r)$ the spatial structure of the beam in the $z = 0$ plane. In the paraxial approximation, the optical modes of the cavity are Gaussian modes with their waist at position $z = 0$ [23]. Assuming the incident beam matched to the fundamental mode of the cavity, the spatial structure $v_0(r)$ of the field is given by

$$v_0(r) = \frac{\sqrt{2/\pi}}{w_0} e^{-r^2/w_0^2}, \tag{7}$$

where w_0 is the optical waist which depends on the geometry of the cavity.

The spatial structure of the reflected field is modified by the mirror motion since the field wave front is distorted and reproduces after reflection the shape of the mirror. At every radial point r of the mirror, the optical path followed by the light is changed by the displacement and the field experiences a local phase shift equal to $2ku(r, z = 0, t)$. The reflected field $E'(r,t)$ is then equal to

$$E'(r,t) = v_0(r)\,\alpha(t)\,e^{-i\omega_0 t} e^{2iku(r,z=0,t)}. \tag{8}$$

Denoting $\{v_n(r)\}$ the basis of Gaussian modes of the cavity, one can write the reflected field as a sum over all modes

$$E'(r,t) = \sum_n \left\langle v_0 e^{2iku(z=0,t)}, v_n \right\rangle v_n(r)\,\alpha(t)\,e^{-i\omega_0 t}, \tag{9}$$

where the brackets stand for the overlap integral in the $z = 0$ plane

$$\langle f, g\rangle = \int_{z=0} \mathrm{d}^2 r\, f(r)\, g(r). \tag{10}$$

Equation (9) shows that the mirror deformation induces a diffusion of the light into all optical modes. This diffusion is however limited by the cavity and it becomes negligible for a non-degenerate and high-finesse cavity. In this case, modes in the sum (9) evolve at a frequency about the resonance frequency ω_0 of the fundamental mode whereas the differences between the resonance frequencies of these modes are large compared to the cavity bandwidth. As a consequence, all modes except the fundamental one are filtered by the cavity bandwidth and cannot propagate in the cavity. One can show that the diffusion in those modes is equivalent to losses for the fundamental mode and that these losses become negligible for a high-finesse cavity [24].

Only the fundamental mode has thus a significant contribution in the sum (9) and we obtain

$$E'(r,t) = \left\langle v_0 e^{2iku(z=0,t)}, v_0 \right\rangle E(r,t). \tag{11}$$

For small displacements u this expression can be approximated to

$$E'(r,t) \approx \left[1 + 2ik\left\langle u(z=0,t), v_0^2\right\rangle\right] E(r,t). \tag{12}$$

The field thus experiences a global phase shift $\psi(t)$ which can be written as

$$\psi(t) = 2k\widehat{u}(t), \tag{13}$$

where $\widehat{u}(t)$ is the displacement of the mirror averaged over the optical waist:

$$\widehat{u}(t) = \left\langle u(z=0,t), v_0^2\right\rangle. \tag{14}$$

The effect of the mirror motion on the intracavity field is thus equivalent to the one obtained in the one-dimensional model. It corresponds to a phase shift given by an equation similar to (1) where the one-dimensional displacement $z(t)$ is replaced by the averaged displacement $\widehat{u}(t)$. All results concerning the effect of the mirror motion on the field can thus be generalized to a mechanical resonator. The light is only sensitive to the displacement $\widehat{u}$ of the mirror which takes into account the spatial overlap between the intracavity field and the mirror motion. In the next section we determine this displacement when the resonator is submitted to the radiation pressure of the intracavity field.

3 Radiation pressure effects

Spatial and frequency characteristics of the acoustic modes depend on the geometry and acoustic properties of the mechanical resonator. To determine the effect of radiation pressure on the mirror motion, it is only necessary to assume that these modes are described by a set of displacements $\{\mathbf{u}_n(\mathbf{r})\}$ which forms a basis of the resonator motion. Each mode n obeys a propagation equation inside the resonator [25]

$$c_\mathrm{t}^2 \Delta \mathbf{u}_n + \left(c_\mathrm{l}^2 - c_\mathrm{t}^2\right) \nabla(\nabla \cdot \mathbf{u}_n) + \Omega_n^2 \mathbf{u}_n = 0, \tag{15}$$

and fulfills the boundary conditions corresponding to a free resonator (see Appendix). In this equation Ω_n is the eigenfrequency of mode n and c_l, c_t are the longitudinal and transverse sound velocities related to the Lamé constants λ and μ of the resonator and to its density ρ by

$$c_\mathrm{l} = \sqrt{(\lambda + 2\mu)/\rho}, \tag{16a}$$

$$c_\mathrm{t} = \sqrt{\mu/\rho}. \tag{16b}$$

Any displacement $\mathbf{u}(\mathbf{r}, t)$ can be expressed as a linear combination of the acoustic modes $\mathbf{u}_n(\mathbf{r})$:

$$\mathbf{u}(\mathbf{r},t) = \sum_n a_n(t)\,\mathbf{u}_n(\mathbf{r}), \tag{17}$$

where $a_n(t)$ is the time-dependent amplitude of mode n. Using this decomposition we can determine the evolution of $\mathbf{u}(\mathbf{r},t)$ when a radiation pressure force is applied on the plane side of the resonator. The total energy E of the resonator is the sum of the kinetic energy, the potential energy and the energy associated with the external force. It can be decomposed in the following form (see the appendix):

$$E=\sum_n\left\{\frac{1}{2}M_n\left(\frac{\mathrm{d}a_n}{\mathrm{d}t}\right)^2+\frac{1}{2}M_n\Omega_n^2a_n^2-\langle\mathbf{F}_{\mathrm{rad}},\mathbf{u}_n\rangle a_n\right\}. \quad (18)$$

M_n represents the mass of the acoustic mode n which is proportional to the volume of the mode inside the resonator:

$$M_n=\rho\int_V \mathrm{d}^3r\,|\mathbf{u}_n(\mathbf{r})|^2. \quad (19)$$

The term $\langle\mathbf{F}_{\mathrm{rad}},\mathbf{u}_n\rangle$ in equation (18) represents the spatial overlap of the scalar product between the radiation pressure $\mathbf{F}_{\mathrm{rad}}$ and the acoustic mode $\mathbf{u}_n$ (Eq. (10)). The radiation pressure is directed along the z-axis and its amplitude $F_{\mathrm{rad}}(r,t)$ at radial position r of the plane side and at time t is related to the intracavity intensity $I(t)=|\alpha(t)|^2$ and to the spatial structure v_0 of the field by

$$F_{\mathrm{rad}}(r,t)=2\hbar kI(t)\,v_0^2(r). \quad (20)$$

The total energy (Eq. (18)) appears as the sum over all modes n of the energies of forced harmonic oscillators. From Hamilton's equations one deduces that each mode amplitude $a_n(t)$ obeys the evolution equation

$$\frac{\mathrm{d}^2a_n}{\mathrm{d}t^2}+\Omega_n^2a_n=\frac{1}{M_n}\langle\mathbf{F}_{\mathrm{rad}},\mathbf{u}_n\rangle. \quad (21)$$

This equation can be written in the Fourier space as

$$a_n[\Omega]=\chi_n[\Omega]\langle\mathbf{F}_{\mathrm{rad}}[\Omega],\mathbf{u}_n\rangle, \quad (22)$$

where $\chi_n[\Omega]=1/M_n\left(\Omega_n^2-\Omega^2\right)$ is the susceptibility in the absence of dissipation for a harmonic oscillator of mass M_n and eigenfrequency Ω_n. The resonator can thus be considered as a set of independent harmonic oscillators, each oscillator being associated with an acoustic mode. These oscillators are driven by an external force which corresponds to the projection of the radiation pressure onto the spatial structure of the acoustic mode in the $z=0$ plane.

Up to now we have assumed that the resonator has no damping. The coupling with a thermal bath can be deduced from the Navier-Stokes equation [25] or from a generalization of the approach used in the one-dimensional model. Each acoustic mode is indeed equivalent to a harmonic oscillator and its damping can be described by a dissipative part added to the mechanical susceptibility and by an additional Langevin force. The susceptibility χ_n of the acoustic mode n has thus an expression similar to the one-dimensional case:

$$\chi_n[\Omega]=\frac{1}{M_n\left(\Omega_n^2-\Omega^2-i\Omega_n^2\Phi_n[\Omega]\right)}, \quad (23)$$

where $\Phi_n[\Omega]$ is the loss angle of mode n. The amplitude a_n of mode n is now given by

$$a_n[\Omega]=\chi_n[\Omega]\left(\langle\mathbf{F}_{\mathrm{rad}}[\Omega],\mathbf{u}_n\rangle+F_{\mathrm{T},n}[\Omega]\right), \quad (24)$$

where $F_{\mathrm{T},n}$ is a Langevin force describing the coupling of mode n with the thermal bath. We assume that these forces are statistically independent of each other and that their spectra are related to the susceptibilities χ_n through fluctuation-dissipation theorem (Eq. (4)). Acoustic modes are then independent and the equation of motion for each amplitude a_n (Eq. (24)) corresponds to the usual expression for a damped harmonic oscillator driven by the projection of the radiation pressure.

We have shown in the previous section that the effect of the mirror deformation on the intracavity field only depends on the longitudinal displacement $\widehat{u}(t)$ which corresponds to the displacement in the $z=0$ plane averaged over the beam waist (Eq. (14)). From equations (14), (17), (20) and (24) this displacement can be expressed in terms of the intracavity intensity I and of thermal fluctuations:

$$\widehat{u}[\Omega]=\chi_{\mathrm{eff}}[\Omega]\left(2\hbar kI[\Omega]+F_{\mathrm{T}}[\Omega]\right). \quad (25)$$

χ_{eff} appears in this equation as an effective susceptibility given by

$$\chi_{\mathrm{eff}}[\Omega]=\sum_n\left\langle v_0^2,u_n\right\rangle^2\chi_n[\Omega], \quad (26)$$

where u_n stands for the z-component of the acoustic mode $\mathbf{u}_n$. The effective susceptibility χ_{eff} is then equal to the sum of all susceptibilities χ_n weighted by the overlap between the acoustic mode and the transverse intensity distribution v_0^2. The force F_{T} in equation (25) is an effective Langevin force related to the forces $F_{\mathrm{T},n}$ of each acoustic modes by

$$F_{\mathrm{T}}[\Omega]=\sum_n\left\langle v_0^2,u_n\right\rangle\frac{\chi_n[\Omega]}{\chi_{\mathrm{eff}}[\Omega]}F_{\mathrm{T},n}[\Omega]. \quad (27)$$

The spectrum of F_{T} can be determined using the independence of the Langevin forces $F_{\mathrm{T},n}$ and their relation to susceptibilities χ_n (Eq. (4)). We find that the force F_{T} is related to χ_{eff} by the fluctuation-dissipation theorem

$$S_{\mathrm{T}}[\Omega]=-\frac{2k_{\mathrm{B}}T}{\Omega}\mathrm{Im}\left(\frac{1}{\chi_{\mathrm{eff}}[\Omega]}\right). \quad (28)$$

This means that the resonator in the absence of external force is in thermodynamic equilibrium at temperature T. Equation (25) also shows that the effective susceptibility χ_{eff} describes both the effects of radiation pressure and of thermal noise represented by the Langevin force F_{T}.

Results obtained here are similar to the ones presented in section 1 for a one-dimensional model. The longitudinal displacement $\widehat{u}$ is related to the intracavity intensity I and to thermal fluctuations by an expression similar to equation (2). The coupling between the resonator and the Gaussian light beam is completely described by the effective susceptibility χ_{eff}. This susceptibility indeed takes

into account all acoustic modes of the resonator and their spatial matching with the light. Treatments made in the framework of the one-dimensional model can thus be generalized by replacing the mirror displacement $z(t)$ by the longitudinal displacement $\widehat{u}(t)$ and the harmonic susceptibility χ by the effective susceptibility $\chi_{\rm eff}$. This is illustrated in the next section where we study the quantum noise reduction of the field reflected by the cavity.

4 Quantum noise reduction

Squeezed-state generation has already been studied for a single-ended cavity containing a pure Kerr medium [18–20] or for a cavity with a harmonically suspended mirror [5]. In this section we extend these results to the case of a mirror coated on a mechanical resonator. We thus consider the system sketched in Figure 1 and we determine the quantum fluctuations of any quadrature of the reflected beam.

For a nearly resonant high-finesse cavity, we have the following relations between the complex amplitudes $\alpha^{\rm in}$, α and $\alpha^{\rm out}$ of the incident, intracavity and reflected fields respectively:

$$\tau\frac{{\rm d}\alpha}{{\rm d}t} = -\left[\gamma - i\Psi(t)\right]\alpha(t) + \sqrt{2\gamma}\alpha^{\rm in}(t), \quad (29a)$$

$$\alpha^{\rm out}(t) = -\alpha^{\rm in}(t) + \sqrt{2\gamma}\alpha(t). \quad (29b)$$

The first relation determines the dynamics of the intracavity field α. τ is the round trip time, γ the damping rate of the cavity ($1-\gamma$ and $\sqrt{2\gamma}$ are respectively the reflection and transmission of the input mirror, with $\gamma \ll 1$) and Ψ is the cavity detuning assumed small compared to 1. Ψ depends on the cavity lentgh and couples the field to the mirror motion. It can be written as the sum of the cavity detuning Ψ_0 without light and the effect of the averaged displacement $\widehat{u}(t)$ (Eq. (13)):

$$\Psi = \Psi_0 + 2k\widehat{u}. \quad (30)$$

The mean cavity detuning $\overline{\Psi}$ differs from Ψ_0 by the contribution due to the mean mirror displacement. Using equation (25) this contribution appears as a non-linear phase shift $\Psi_{\rm NL}$ related to the mean intracavity intensity $\overline{I}$ by an expression similar to equation (5):

$$\overline{\Psi} = \Psi_0 + \Psi_{\rm NL}, \quad (31a)$$

$$\Psi_{\rm NL} = 4\hbar k^2 \chi_{\rm eff}[0]\,\overline{I}. \quad (31b)$$

The behavior of the mean fields is thus the same as the one for a cavity containing a pure Kerr medium. In particular the non-linear phase shift is responsible for the bistability of the system [5]. From equations (29) the mean intracavity intensity is related to the incident power $P^{\rm in}$ by

$$\left(\gamma^2 + \overline{\Psi}^2\right)\overline{I} = 2\gamma\frac{\lambda}{hc}P^{\rm in}. \quad (32)$$

Due to the intensity dependence of the non-linear phase shift, one can obtain different intracavity intensities for a given incident power. This bistable behavior can be characterized by the inverse slope $\sigma = {\rm d}P^{\rm in}/{\rm d}\overline{I}$ of the curve giving the intracavity intensity as a function of the incident power. σ is proportional to

$$\sigma \propto \gamma^2 + \overline{\Psi}^2 + 2\overline{\Psi}\Psi_{\rm NL}. \quad (33)$$

The positive, negative, and null values of σ correspond, respectively, to stable branches, unstable branch, and turning points [20].

To determine the fluctuations $\delta\alpha^{\rm out}[\Omega]$ of the field reflected by the cavity, we use the semiclassical method in which quantum fluctuations are treated as classical random variables associated with the Wigner distribution [26–28]. Their evolution is deduced from the classical equations (29) linearized around the mean state. We obtain

$$\left(\gamma - i\overline{\Psi} - i\Omega\tau\right)\delta\alpha[\Omega] = \sqrt{2\gamma}\delta\alpha^{\rm in}[\Omega] + i\overline{\alpha}\delta\Psi[\Omega], \quad (34a)$$

$$\delta\alpha^{\rm out}[\Omega] = \sqrt{2\gamma}\delta\alpha[\Omega] - \delta\alpha^{\rm in}[\Omega], \quad (34b)$$

$$\overline{\alpha}\delta\Psi[\Omega] = \widetilde{\chi}_{\rm eff}[\Omega]\,\Psi_{\rm NL}\left(\delta\alpha[\Omega] + \delta\alpha^*[\Omega]\right) + 2k\overline{\alpha}\chi_{\rm eff}[\Omega]\,F_{\rm T}[\Omega], \quad (34c)$$

where $\overline{\alpha}$ is the mean intracavity field and $\widetilde{\chi}_{\rm eff}[\Omega] = \chi_{\rm eff}[\Omega]/\chi_{\rm eff}[0]$ is the mechanical susceptibility normalized to 1 at zero frequency. We deduce from these equations the input-output relations for the field which give the output field fluctuations $\delta\alpha^{\rm out}$ as a function of the input field fluctuations $\delta\alpha^{\rm in}$ and of the Langevin force $F_{\rm T}$:

$$\delta\alpha^{\rm out}[\Omega] = \left\{c_1[\Omega]\,\delta\alpha^{\rm in}[\Omega] + c_2[\Omega]\,\delta\alpha^{\rm in*}[\Omega] + c_{\rm T}[\Omega]\,F_{\rm T}[\Omega]\right\}, \quad (35)$$

where the coefficients $c_1[\Omega]$, $c_2[\Omega]$ and $c_{\rm T}[\Omega]$ depend on the system parameters

$$c_1[\Omega] = \frac{1}{\Delta}\left\{\left(\gamma + i\overline{\Psi}\right)\left(\gamma + i\overline{\Psi} + 2i\Psi_{\rm NL}\widetilde{\chi}_{\rm eff}[\Omega]\right) + (\Omega\tau)^2\right\}, \quad (36a)$$

$$c_2[\Omega] = \frac{2i}{\Delta}\gamma\Psi_{\rm NL}\widetilde{\chi}_{\rm eff}[\Omega], \quad (36b)$$

$$c_{\rm T}[\Omega] = \frac{2i}{\Delta}\sqrt{2\gamma}k\overline{\alpha}\left(\gamma + i\overline{\Psi} - i\Omega\tau\right)\chi_{\rm eff}[\Omega], \quad (36c)$$

$$\Delta = (\gamma - i\Omega\tau)^2 + \overline{\Psi}^2 + 2\overline{\Psi}\Psi_{\rm NL}\widetilde{\chi}_{\rm eff}[\Omega]. \quad (36d)$$

From these relations one can determine the spectrum $S_\theta^{\rm out}$ for any quadrature $\alpha_\theta^{\rm out}$ of the reflected field defined by

$$\delta\alpha_\theta^{\rm out}[\Omega] = e^{-i\theta}\delta\alpha^{\rm out}[\Omega] + e^{i\theta}\delta\alpha^{\rm out*}[\Omega], \quad (37a)$$

$$\overline{\delta\alpha_\theta^{\rm out}[\Omega]\,\delta\alpha_\theta^{\rm out}[\Omega']} = 2\pi\delta(\Omega + \Omega')\,S_\theta^{\rm out}[\Omega], \quad (37b)$$

where the bar stands for the average over the Wigner distribution. Equations (35) and (36) show that the quantum properties of the reflected field only depend on a few parameters. The cavity is characterized by the damping γ which is related to its finesse $\mathcal{F} = \pi/\gamma$, by the cavity bandwidth $\Omega_{\rm cav} = \gamma/\tau$ and by the mean detuning $\overline{\Psi}$. The mirror motion is described by the non-linear phase shift

$\Psi_{\rm NL}$ and by the frequency dependence $\widetilde{\chi}_{\rm eff}$ of the mechanical response. The last coefficient $c_{\rm T}$ describes thermal effects associated with the Brownian motion of the mirror. To obtain quantitative values for the noise reduction, it is necessary to determine the mechanical response of the resonator which may depend on its geometry. We study in the next section the case of a plano-convex resonator.

Note finally that the differences with a pure Kerr effect are only due to the frequency dependence of the mechanical response and to thermal fluctuations. One gets the usual expressions for a Kerr medium by taking $\widetilde{\chi}_{\rm eff}[\Omega]=1$ and $F_{\rm T}[\Omega]=0$ in equations (35) and (36).

5 Optomechanical coupling with a plano-convex resonator

We consider in this section that the resonator has a plano-convex geometry with a mirror coated on its plane side (Fig. 1). We first determine the analytical expression of the effective susceptibility. We then study the quantum noise reduction of the field reflected by the cavity and we finally derive the effective mass associated with the optomechanical coupling.

5.1 Effective susceptibility

If the resonator thickness h_0 is much smaller than the curvature radius R of the convex side, the propagation equation (15) can be solved using a paraxial approximation and one gets analytical expressions for the acoustic modes corresponding to Gaussian modes [29]. Only modes that have a non-zero overlap with the light intensity contribute to the effective susceptibility (Eq. (26)). As a consequence we disregard shear modes which induce no longitudinal displacement and we consider only the compression modes that have a cylindrical symmetry. Those modes are defined by two integers, a longitudinal index n and a transverse index p, and the longitudinal displacement $u_{n,p}(r,z)$ at point of radial coordinate r and axial coordinate z is given by

$$u_{n,p}(r,z)=e^{-r^2/w_n^2}L_p\left(2r^2/w_n^2\right)\cos\left(\frac{n\pi}{h(r)}z\right). \quad (38)$$

$u_{n,p}$ is composed of a transverse Gaussian structure with a waist w_n, a transverse Laguerre polynomial L_p and a cosine in the propagation direction. $h(r)$ is the resonator thickness at radial position r given by

$$h(r)\approx h_0-\frac{r^2}{2R}. \quad (39)$$

The acoustic waists w_n depend on the longitudinal index n:

$$w_n^2=\frac{2h_0}{n\pi}\sqrt{Rh_0}. \quad (40)$$

The acoustic modes $u_{n,p}$ are solution of the propagation equation inside the resonator and each mode evolves with an eigenfrequency $\Omega_{n,p}$ given by

$$\Omega_{n,p}^2=\Omega_M^2\left[n^2+\frac{2}{\pi}\sqrt{\frac{h_0}{R}}n\,(2p+1)\right], \quad (41)$$

where $\Omega_{\rm M}=\pi c_{\rm l}/h_0$.

One can now derive an analytical expression for the effective susceptibility as an infinite sum over all modes $\{n,p\}$ (Eq. (26)). In this expression the mass M_n of the acoustic mode $\{n,p\}$ (Eq. (19)) only depends on the longitudinal index n and is equal to

$$M_n=\frac{\pi}{4}\rho h_0 w_n^2. \quad (42)$$

This mass is proportional to the volume of the acoustic mode and is smaller than the total mass of the resonator. We can also derive the overlap between acoustic and optical modes

$$\left\langle v_0^2,u_{n,p}\right\rangle=\frac{2w_n^2}{2w_n^2+w_0^2}\left(\frac{2w_n^2-w_0^2}{2w_n^2+w_0^2}\right)^p. \quad (43)$$

The overlap only depends on the ratio w_n/w_0 between acoustic and optical waists.

We assume for simplicity that the loss angles $\Phi_{n,p}[\Omega]$ are the same for all modes and are constant in frequency. As a consequence these loss angles are simply related to the quality factor Q of the fundamental mode $\{1,0\}$ of the resonator by

$$\Phi_{n,p}[\Omega]\equiv 1/Q. \quad (44)$$

These equations allow to compute any parameters of the optomechanical coupling. For example the non-linear phase shift $\Psi_{\rm NL}$ is related through equation (31b) to the effective susceptibility at zero frequency which is given by

$$\chi_{\rm eff}[0]=\sum_{n,p}\frac{\left\langle v_0^2,u_{n,p}\right\rangle^2}{M_n\Omega_{n,p}^2}. \quad (45)$$

This sum can be numerically computed. In the following we consider a small plano-convex resonator of thickness h_0 equal to 1.5 mm and with a curvature radius R of the convex side equal to 150 mm. For these values the acoustic waist w_1 of the fundamental mode is equal to 3.8 mm. It is much larger than the optical waist w_0 which is typically of the order of 100 μm for a cavity of 1 mm long with a curvature radius of the input mirror equal to 1 m. As a consequence the overlap (43) slowly decreases with the mode indices $\{n,p\}$ and it is necessary to sum over more than 10^6 modes to obtain a precision better than 10^{-3}.

5.2 Optimum squeezing

We determine now the optimum squeezing $S_{\rm opt}[\Omega]$ of the reflected field, that is the minimum value of the spectrum

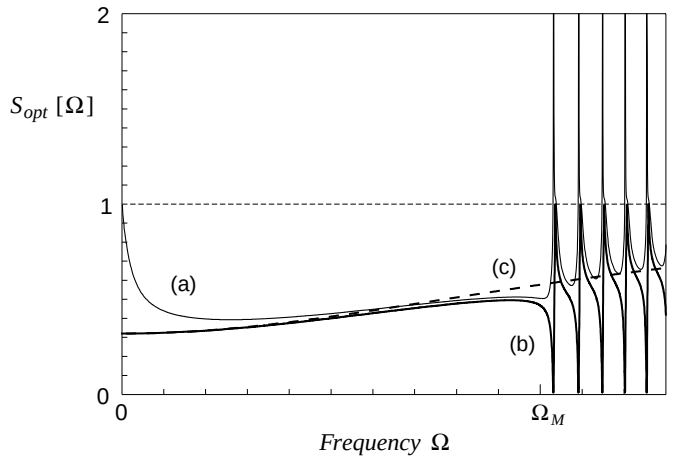

Fig. 2. Optimum noise spectrum $S_{\rm opt}\,[\Omega]$ of the reflected field as a function of frequency. Curves (a) and (b) are obtained at $T = 4$ K and at zero temperature, respectively. The dashed curve (c) corresponds to the pure Kerr effect for the same parameters ($\overline{\Psi} = -0.2\gamma$, $\Psi_{\rm NL} = 0.28\gamma$).

$S_\theta^{\rm out}\,[\Omega]$ obtained at every frequency Ω by scanning the quadrature θ. We assume that the mechanical resonator is made of silica (density $\rho = 2200$ kg/m^3, longitudinal sound velocity $c_{\rm l} = 5960$ m/s). Its fundamental resonance frequency $\Omega_{\rm M}/2\pi$ is then equal to 2 MHz and we take a quality factor Q of 10^6. The cavity is characterized by its damping γ equal to 10^{-5} (cavity finesse $\mathcal{F} = 3 \times 10^5$) and its working point is defined by the mean detuning $\overline{\Psi}$ chosen equal to -0.2γ. We also assume that the cavity bandwidth $\Omega_{\rm cav} = \gamma/\tau$ is equal to $\Omega_{\rm M}$ and that the optical wavelength λ is equal to 800 nm.

To determine the non-linear phase shift $\Psi_{\rm NL}$, we compute the effective susceptibility $\chi_{\rm eff}\,[0]$ at zero frequency from equation (45). We obtain $\chi_{\rm eff}\,[0] = 1.4 \times 10^{-8}$ m/N for an optical waist w_0 of 200 μm. From equations (31b) and (32) one then gets a non-linear phase shift $\Psi_{\rm NL}$ equal to 0.28γ for an incident power $P^{\rm in}$ of 10 mW. Note that these values correspond to a positive slope σ of the bistability curve, equal to $0.93\gamma^2$ (Eq. (33)). The working point is thus on a stable branch of the bistability curve.

Figure 2 shows the optimum squeezing $S_{\rm opt}\,[\Omega]$ as a function of frequency. Curve (a) is obtained at a temperature of 4 K. The noise spectrum exhibits a strong reduction over a wide frequency range from zero up to the first resonance frequency of the resonator. For higher frequencies the spectrum shows an excess noise at every mechanical resonance frequencies.

It is instructive to compare this spectrum to the ones obtained at zero temperature (curve b) and for a pure Kerr effect with the same parameters $\Psi_{\rm NL}$ and $\overline{\Psi}$ (curve c). At low frequencies ($\Omega < \Omega_{\rm M}$) the noise spectrum at zero temperature (curve b) is similar to the one obtained with a Kerr effect (curve c). The whole effect of the mechanical motion can be interpreted as a non-linear phase shift $\Psi_{\rm NL}$ for the light. At finite temperatures (curve a), the Brownian motion of the mirror slightly increases the noise. Note that this effect depends on the dissipation mechanisms in the resonator. In particular the large increase at zero frequency is due to the choice of a constant loss angle. One would obtain less thermal noise in the framework of a Navier-Stockes model for which the loss angle is a linear function of frequency.

For higher frequencies ($\Omega > \Omega_{\rm M}$) the dynamics of the mechanical resonator plays an important role. At zero temperature (curve b) we observe a series of dispersion-shaped resonances centered on every mechanical resonance $\Omega_{n,p}$, with an important noise reduction for frequencies slightly below each resonance. Thermal noise however masks this behavior since the Brownian motion is concentrated around the mechanical resonances and increases the noise (curve a).

To summarize this discussion, it appears that the most interesting frequency domain for quantum noise reduction is the low-frequency domain ($\Omega < \Omega_{\rm M}$). For sufficiently low temperature the noise behavior is similar to the one obtained with a pure Kerr effect and it mainly depends on the non-linear phase shift $\Psi_{\rm NL}$. More precisely the frequency dependence of the noise spectrum roughly corresponds to a low-pass filtering due to the cavity bandwidth and the amplitude of noise reduction becomes important near the bistability turning points [20]. To reach these points the non-linear phase shift $\Psi_{\rm NL}$ must be large enough, that is of the order of γ.

5.3 Effective mass

The non-linear phase shift depends on the mechanical and optical properties of the system. In particular it is related to the spatial overlap between the various acoustic modes and the light (Eq. (45)). Figure 3 shows the optimum squeezing $S_{\rm opt}\,[\Omega]$ for different values of the optical waist w_0 (400, 200 and 100 μm), the other parameters being identical to the ones of Figure 2 ($P_{\rm in} = 10$ mW, $\gamma = 10^{-5}$, $\overline{\Psi} = -0.2\gamma$, $T = 4$ K and $Q = 10^6$). For each curve we have computed the effective susceptibility $\chi_{\rm eff}\,[0]$ at zero frequency and we have determined the non-linear phase shift $\Psi_{\rm NL}$. Curves (a) to (c) correspond to increasing non-linear phase shifts (0.11γ, 0.28γ and 0.62γ, respectively) and to decreasing slopes of the bistability curve ($0.99\gamma^2$, $0.93\gamma^2$ and $0.79\gamma^2$, respectively).

One observes a drastic increase of the noise reduction when w_0 decreases. This result can be interpreted as a reduction of the effective mass associated with the optomechanical coupling. Quantum effects observed in Figures 2 and 3 in the low-frequency domain are actually similar to the ones obtained with a harmonically suspended mirror. The effective susceptibility of the resonator is thus equivalent at low frequency to the susceptibility of a single harmonic oscillator with a resonance frequency $\Omega_{\rm M}$. The mass of this equivalent pendulum is however different from the total mass of the resonator since it depends on the spatial matching with the light. This effective mass $M_{\rm eff}$ can be deduced from a comparison between the effective susceptibility $\chi_{\rm eff}\,[0]$ at zero frequency and the one

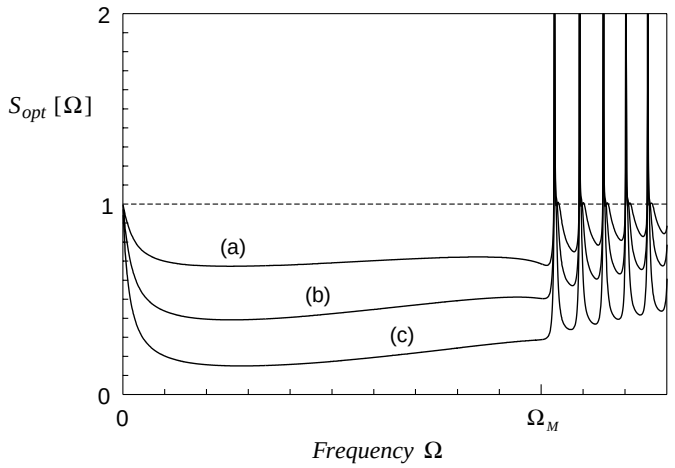

Fig. 3. Optimum noise spectra $S_{\rm opt}\,[\Omega]$ of the reflected field for different optical waists w_0. Curves (a) to (c) correspond respectively to 400, 200 and 100 μm.

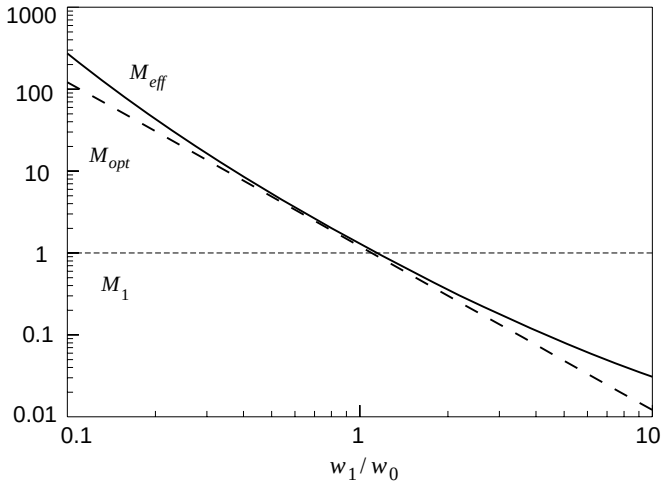

Fig. 4. Effective mass $M_{\rm eff}$ of the resonator as a function of the ratio between fundamental acoustic and optical waists. The dashed curve represents the optical mass $M_{\rm opt}$ related to the volume of the resonator illuminated by the light. The vertical scale is normalized to the mass M_1 of the fundamental acoustic mode (37 mg).

of a harmonic oscillator (Eqs. (3) and (45)):

$$\frac{1}{M_{\rm eff}\Omega_{\rm M}^2} = \sum_{n,p} \frac{\left\langle v_0^2, u_{n,p}\right\rangle^2}{M_{n,p}\Omega_{n,p}^2}. \tag{46}$$

The effective mass is related to the masses of all acoustic modes coupled to the light. The number of acoustic modes contributing to the sum strongly depends on the light waist. The typical variation length of the Laguerre polynomial $L_p\left(2r^2/w_n^2\right)$ in the spatial structure of the acoustic mode $\{n,p\}$ is $w_n/\sqrt{p}$. The overlap $\left\langle v_0^2, u_{n,p}\right\rangle$ is thus equal to 1 as long as w_0 is much smaller than $w_n/\sqrt{p}$ (Eq. (43)). For a given value of n, the number of transverse modes which contribute to the effective mass is proportional to w_1^2/nw_0^2 and it increases when w_0 decreases. As a consequence the mass becomes smaller and quantum effects of radiation pressure become larger.

From equations (41) to (43) one can express the effective mass as a function of the waists w_1, w_0 and of the mass M_1 of the fundamental mode:

$$\frac{M_1}{M_{\rm eff}} = \sum_{n,p} \frac{4w_1^4}{\left(2w_1^2+nw_0^2\right)^2}\left(\frac{2w_1^2-nw_0^2}{2w_1^2+nw_0^2}\right)^{2p} \times \frac{1}{n+\dfrac{2}{\pi}\sqrt{\dfrac{h_0}{R}}\,(2p+1)}. \tag{47}$$

The solid line in Figure 4 shows the variation of the effective mass as a function of the ratio w_1/w_0 for a resonator of thickness $h_0 = 1.5$ mm and of curvature radius $R = 150$ mm. It clearly appears that this mass decreases with the optical waist and very small values can be reached. The mass M_1 of the fundamental mode is equal to 37 mg (Eq. (42)) and one gets an effective mass of 1 mg for an optical waist equal to $w_1/10$ (380 μm) and a mass of 0.2 mg for a waist of 100 μm. Such small values would be very difficult to obtain with a harmonically suspended mirror for which the mass associated with the global motion is the total mass of the mirror.

One can get a simple physical insight into the effective mass in the case of a resonator thickness much smaller than the curvature radius of the convex side ($h_0 \ll R$). We can then assume that the transverse modes of the resonator are degenerate, that is the resonance frequencies $\Omega_{n,p}$ are independent of p. The sum over p in equation (47) is a simple geometric sum and one gets an estimate $M_{\rm opt}$ of the effective mass given by

$$\frac{M_1}{M_{\rm opt}} = \frac{w_1^2}{2w_0^2}\sum_n \frac{1}{n^2} = \frac{\pi^2}{12}\left(\frac{w_1}{w_0}\right)^2. \tag{48}$$

Using the expression of M_1 (Eq. (42)), we finally obtain

$$M_{\rm opt} = \frac{12}{\pi^2}\left(\frac{\pi}{4}\rho h_0 w_0^2\right). \tag{49}$$

The term in brackets corresponds to the mass of the part of the resonator illuminated by the light beam. This optical mass is a good approximation of the effective mass $M_{\rm eff}$ as shown by the dashed curve in Figure 4. We have thus shown that the effect of the resonator motion on the light is equivalent to the one of a harmonically suspended mirror of mechanical resonance frequency $\Omega_{\rm M}$ and of mass related to the light spot size. This mass can of course become very small for a small optical waist.

6 Conclusion

We have studied the quantum effects due to radiation pressure in a high-finesse cavity with a mirror coated on a mechanical resonator. We have shown that the optomechanical coupling between the Gaussian laser beam and

the acoustic modes of the resonator leads to a non-linear phase shift for the light. This phase shift is related to the intracavity intensity through an effective susceptibility which takes into account all the acoustic modes and their coupling to the light. This susceptibility also describes the effect on the light of the Brownian motion of the mirror.

We have studied the quantum noise reduction of the field reflected by the cavity. This quantum effect mainly depends on the behavior of the non-linear phase shift at low frequency. In this frequency domain the mechanical response of the resonator can be approximated to a harmonic response. The effect of optomechanical coupling is then equivalent to the one obtained with a harmonically suspended mirror of resonance frequency equal to the fundamental resonance frequency of the resonator. The mass of this equivalent pendulum is however smaller than the total mass of the mirror, thus enhancing the optomechanical coupling. We have shown that for a plano-convex resonator this effective mass is of the order of the optical mass which corresponds to the volume of the resonator illuminated by the light. The effective mass can be two or three orders of magnitude smaller than the total mass of the mirror and large quantum effects are obtained for a reasonable input power when the optical waist is small enough.

This drastic decrease of the effective mass seems to be a specific behavior of the plano-convex geometry. The effective susceptibility of a cylindrical mirror has already been determined at low frequency for the study of thermal effects in gravitational-wave detectors [13,14]. The reduction of the effective mass does not exceed a factor 10 below the total mass of the mirror. The plano-convex geometry thus allows to get simultaneously a high resonance frequency and a very small mass so that large quantum noise reduction can be obtained over a wide frequency range. One can of course obtain significant non-linear phase shifts with a cylindrical mirror but the fundamental resonance frequency is very low.

Finally, we have only studied in this paper the quantum noise reduction of the field reflected by the cavity. Similar results would however be obtained for other quantum effects of radiation pressure such as the possibility of quantum non-demolition measurement of light intensity [10] or the quantum limit in interferometric measurements. For example, it has been shown that the quantum limit for measurement sensitivity is proportional to the susceptibility characterizing the mirror motion [2]. The quantum limit induced by internal acoustic modes is thus proportional to the effective susceptibility studied in this paper. In particular the sensitivity is reduced if mirrors have small effective masses.

We gratefully acknowledge F. Bondu for the program *CYPRES* used to compute the effective susceptibility of a cylindrical mirror. Y. Hadjar acknowledges a fellowship from the *Association Louis de Broglie d'Aide à la Recherche*.

Appendix: Propagation equation for a resonator submitted to radiation pressure

In this appendix we derive the evolution equation of the acoustic modes for a resonator submitted to a radiation pressure force. This derivation is actually similar to the phonon decomposition in the presence of an external force.

The evolution equation of any displacement $\mathbf{u}(\mathbf{r},t)$ can be deduced from the Lagrangian $L = T - U$ where the kinetic energy T and the potential energy U are equal to [25]

$$T = \int_V \frac{1}{2}\rho \left|\frac{\partial \mathbf{u}}{\partial t}\right|^2 \mathrm{d}^3 r, \tag{A.1a}$$

$$U = \sum_{ij} \int_V \frac{1}{2}\sigma_{ij} u_{ij} \mathrm{d}^3 r, \tag{A.1b}$$

where ρ is the density of the resonator. The strain tensor u_{ij} is given by

$$u_{ij} = \frac{1}{2}\left(\frac{\partial u_j}{\partial x_i} + \frac{\partial u_i}{\partial x_j}\right), \tag{A.2}$$

where u_i $(i = 1, 2, 3)$ are the Cartesian components of the displacement $\mathbf{u}(\mathbf{r},t)$ at point $\mathbf{r}$ of Cartesian coordinates x_i. The stress tensor σ_{ij} is related to the strain tensor u_{ij} by Hooke's law

$$\sigma_{ij} = 2\mu u_{ij} + \lambda \nabla \cdot \mathbf{u} \delta_{ij}, \tag{A.3}$$

where λ and μ are the Lamé constants of the resonator. We deduce from the Lagrange equations the propagation equation of $\mathbf{u}(\mathbf{r},t)$ in the resonator

$$\rho \frac{\partial^2 \mathbf{u}}{\partial t^2} = \mu \Delta \mathbf{u} + (\lambda + \mu) \nabla (\nabla \cdot \mathbf{u}). \tag{A.4}$$

For a free resonator the constraint tensor σ_{ij} at every point $\mathbf{r}$ of the surface must satisfy the following condition for any Cartesian index i:

$$\sum_j \sigma_{ij}(\mathbf{r},t)\, n_j = 0, \tag{A.5}$$

where $\mathbf{n}$ is the normal vector at point $\mathbf{r}$.

Acoustic modes are defined as monochromatic solutions $\mathbf{u}_n(\mathbf{r})\, e^{-i\Omega_n t}$ of equations (A.4) and (A.5). Each acoustic mode can be decomposed into longitudinal and transverse components denoted $\mathbf{u}_n^{\mathrm{l}}$ and $\mathbf{u}_n^{\mathrm{t}}$, respectively and defined by

$$\nabla \times \mathbf{u}_n^{\mathrm{l}} = 0,\ \nabla \cdot \mathbf{u}_n^{\mathrm{t}} = 0. \tag{A.6}$$

These components obey the following propagation equations:

$$\Delta \mathbf{u}_n^{\mathrm{l}} + \frac{\Omega_n^2}{c_{\mathrm{l}}^2}\mathbf{u}_n^{\mathrm{l}} = 0, \tag{A.7a}$$

$$\Delta \mathbf{u}_n^{\mathrm{t}} + \frac{\Omega_n^2}{c_{\mathrm{t}}^2}\mathbf{u}_n^{\mathrm{t}} = 0, \tag{A.7b}$$

where c_l and c_t are the longitudinal and transverse sound velocities (Eq. (16)).

Since the set $\{\mathbf{u}_n(\mathbf{r})\}$ of acoustic modes forms a basis for the solutions of equations (A.4) and (A.5), any displacement $\mathbf{u}(\mathbf{r},t)$ can be decomposed on these modes with time-dependent amplitudes $a_n(t)$ (Eq. (17)). We now determine the total energy $E = T + U$ associated with this displacement. From equation (A.1a) the kinetic energy T is equal to

$$T = \sum_n \frac{1}{2} M_n \left(\frac{\mathrm{d}a_n}{\mathrm{d}t}\right)^2, \tag{A.8}$$

where M_n is the mass of mode u_n (Eq. (19)). The potential energy U is given by equation (A.1b) and can be written as

$$U = \sum_{i,j} \frac{1}{2} \int_V \mathrm{d}^3 r \left[\frac{\partial(\sigma_{ij} u_j)}{\partial x_i} - \frac{\partial \sigma_{ij}}{\partial x_i} u_j\right]. \tag{A.9}$$

The first term can be transformed into a surface integral which is equal to zero for a displacement satisfying the boundary condition (A.5). Using the decomposition of $\mathbf{u}_n$ into longitudinal and transverse components and the propagation equations (A.7), one then gets

$$U = \sum_n \frac{1}{2} M_n \Omega_n^2 \left[a_n(t)\right]^2. \tag{A.10}$$

The total energy E is finally equal to

$$E = \sum_n \left\{\frac{1}{2} M_n \left(\frac{\mathrm{d}a_n}{\mathrm{d}t}\right)^2 + \frac{1}{2} M_n \Omega_n^2 \left[a_n(t)\right]^2\right\}, \tag{A.11}$$

and appears as the sum of the energies of free harmonic oscillators.

Up to now we have assumed that the resonator is free from any external constraint. In the presence of radiation pressure there is an additional contribution to the energy corresponding to the work of internal constraints opposed to the external force

$$W = -\int_{z=0} \mathrm{d}^2 r \mathbf{F}_\mathrm{rad}(\mathbf{r},t) \cdot \mathbf{u}(\mathbf{r},t). \tag{A.12}$$

The total energy E is then equal to

$$E = \sum_n \left\{\frac{1}{2} M_n \left(\frac{\mathrm{d}a_n}{\mathrm{d}t}\right)^2 + \frac{1}{2} M_n \Omega_n^2 \left[a_n(t)\right]^2 - \langle \mathbf{F}_\mathrm{rad}, \mathbf{u}_n \rangle a_n(t)\right\}, \tag{A.13}$$

where $\langle \mathbf{F}_\mathrm{rad}, \mathbf{u}_n \rangle$ is the overlap integral in the $z = 0$ plane of the scalar product between the radiation pressure and the acoustic mode u_n (Eq. (10)). We have thus shown that the total energy is the sum over all modes of the energies of forced harmonic oscillators. The evolution equation (21) for each mode amplitude a_n is then deduced from Hamilton's equations.

References

1. C.M. Caves, Phys. Rev. D **23**, 1693 (1981).
2. M.T. Jaekel, S. Reynaud, Europhys. Lett. **13**, 301 (1990).
3. V.B. Braginsky, Yu.I. Vorontsov, Usp. Fiz. Nauk. **114**, 41 (1974) (Sov. Phys. Usp. **17**, 644 (1975)); V.B. Braginsky, Yu.I. Vorontsov, Usp. Fiz. Nauk. **114**, 41 (1974) (Sov. Phys. Usp. **17**, 644 (1975)).
4. A. Heidmann, S. Reynaud, Phys. Rev. A **50**, 4237 (1994).
5. C. Fabre, M. Pinard, S. Bourzeix, A. Heidmann, E. Giacobino, S. Reynaud, Phys. Rev. A **49**, 1337 (1994).
6. S. Mancini, V.I. Manko, P. Tombesi, Phys. Rev. A **55**, 3042 (1997).
7. S. Bose, K. Jacobs, P.L. Knight, Phys. Rev. A **56**, 4175 (1997).
8. K. Jacobs, P. Tombesi, M.J. Collett, D.F. Walls, Phys. Rev. A **49**, 1961 (1994).
9. M. Pinard, C. Fabre, A. Heidmann, Phys. Rev. A **51**, 2443 (1995).
10. A. Heidmann, Y. Hadjar, M. Pinard, Appl. Phys. B **64**, 173 (1997).
11. C. Bradaschia *et al.*, Nucl. Inst. Meth. A **289**, 518 (1990).
12. A. Abramovici *et al.*, Science **256**, 325 (1992).
13. F. Bondu, J.Y. Vinet, Phys. Lett. A **198**, 74 (1995).
14. A. Gillespie, F. Raab, Phys. Rev. D **52**, 577 (1995).
15. Y. Levin, Phys. Rev. D **57**, 659 (1998).
16. F. Bondu, P. Hello, J.Y. Vinet, Phys. Lett. A **246**, 227 (1998).
17. L. Landau, E. Lifshitz, *Course of Theoretical Physics: Statistical Physics* (Pergamon, New York, 1958), chapt. 12.
18. M.J. Collett, D.F. Walls, Phys. Rev. A **32**, 2887 (1985).
19. R.M. Shelby, M.D. Levenson, D.F. Walls, A. Aspect, G.J. Milburn, Phys. Rev. A **33**, 4008 (1986).
20. S. Reynaud, C. Fabre, E. Giacobino, A. Heidmann, Phys. Rev. A **40**, 1440 (1989).
21. P. Alsing, G.J. Milburn, D.F. Walls, Phys. Rev. A **37**, 2970 (1988).
22. P. Grangier, J.F. Roch, S. Reynaud, Opt. Commun. **72**, 387 (1989).
23. H.W. Kogelnik, T. Li, Appl. Opt. **5**, 1550 (1966).
24. J.M. Courty, A. Lambrecht, Phys. Rev. A **54**, 5243 (1996).
25. L. Landau, E. Lifshitz, *Course of Theoretical Physics: Theory of Elasticity* (Pergamon, New York, 1958).
26. S. Reynaud, A. Heidmann, Opt. Commun. **71**, 209 (1989).
27. S. Reynaud, A. Heidmann, E. Giacobino, C. Fabre, in *Progress in Optics XXX*, edited by E. Wolf (North-Holland, Amsterdam, 1992), p. 1.
28. C. Fabre, S. Reynaud, in *Fundamental Systems in Quantum Optics*, 1990 Les Houches Lectures, edited by J. Dalibard, J.M. Raymond, J. Zinn-Justin (North-Holland, Amsterdam, 1992), p. 675.
29. C.J. Wilson, J. Phys. D: Appl. Phys. **7**, 2449 (1974).